PNAS

Supporting Information for

Modulation of xanthophyll cycle impacts biomass productivity in the marine microalga *Nannochloropsis*

Giorgio Perin[1,§], Alessandra Bellan[1,§], Tim Michelberger[1], Dagmar Lyska[2], Setsuko Wakao[2], Krishna K. Niyogi[2,3], Tomas Morosinotto[1,*]

1. Department of Biology, University of Padova, Via Ugo Bassi 58/B, 35131, Padova, Italy
2. Molecular Biophysics and Integrated Bioimaging Division Lawrence Berkeley National Laboratory, Berkeley, CA 94720, USA
3. Howard Hughes Medical Institute, Department of Plant and Microbial Biology, University of California, Berkeley, CA 94720-3102

*Corresponding author: Tomas Morosinotto, Department of Biology, University of Padova, Via Ugo Bassi 58/B, 35131, Padova, Italy. Phone: +390498277484

Email: tomas.morosinotto@unipd.it

This PDF file includes:

Supporting text
Figures S1 to S13
Tables S1 to S6

§ Equal contribution

Supporting Information Text

Supporting results

Impact of alterations in the xanthophyll cycle on photosynthetic functionality

The Chl fluorescence kinetics after exposure to increasing light intensities was also monitored for all strains to assess in more detail the impact of alterations in the xanthophyll cycle on the functionality of the photosynthetic machinery. This confirmed a small reduction in NPQ of the ZEP over-expressor with respect to WT, while *vde KO* and *lhcx1 KO* showed a total absence of response (Supplementary figure S5a). In all strains, the photosynthetic electron transport (ETR) increased as a function of light intensity, reaching saturation at approx. 500 µmol photons m^{-2} s^{-1}. When light intensity further increased, ETR decreased suggesting cells cannot efficiently process all the received photons (Supplementary figure S5b). In *vde KO* ETR values remained lower than the parental strain. *lhcx1 KO* strain showed instead an ETR higher than WT at saturating light intensities. The greatest increase in ETR was observed for the *ZEP* OE, that also reached saturation at higher light intensities than the parental strain (Supplementary figure S5b).

The fluorescence parameter qL can also be exploited to assess photochemical activity: when all reaction centers are available for photochemical reactions its value is 1, whilst it trends to 0 when the photochemical capacity is saturated (1). Both *vde KO* and *lhcx1 KO* showed a faster reduction of qL as the light intensity increases, suggesting their reactions centers were more easily saturated. The *ZEP* OE, instead, showed a higher photochemical activity than the parental strains at saturating light intensities (Supplementary figure S5c). This is also confirmed by the trend of PSII quantum yield of samples illuminated with increasing irradiances, where the *ZEP* OE showed a slower reduction of PSII activity with respect to the parental strain (Supplementary figure S5d).

The photosynthetic electron transport activity was assessed also using an alternative method, measuring the oxygen evolution upon exposure to increasing light intensity. Whilst no difference between the *ZEP* OE and the parental strain was observed, both *vde KO* and *lhcx1 KO* showed instead a strong reduction (Supplementary figure S5e), highlighting the importance of NPQ and xanthophyll cycle to preserve photosynthetic functionality in cells exposed to over-saturating irradiances.

Supporting materials and methods

Strains

It is worth mentioning here that the species *Nannochloropsis gaditana* was officially re-named *Microchloropsis gaditana* (https://www.algaebase.org/search/species/detail/?species_id=157330). A couple of studies in the past years indeed led to a proposed revision in the nomenclature of the genus *Nannochloropsis* (2, 3), with the description of a new species (i.e. *Nannochlorospis australis*) and the shifting of *Nannochloropsis gaditana* and *Nannochloropsis salina* into a new genus, *Microchloropsis*. Despite the formal decision of using the new nomenclature, the scientific community working with marine microalgae species is still mostly using the term *Nannochloropsis*, which is officially considered an homotypic synonym (https://www.algaebase.org/search/species/detail/?species_id=157330).

Therefore, in this work we preferred to use the original species name to avoid i) confusion in the readers who are likely not to be familiar with this change and ii) the presentation of results from the same strain under different species name in papers a few years apart.

RNA extraction

Total RNA was extracted from semicontinuous cultures over >6 months of sampling campaigns, according to (4). Cells were collected via centrifugation and frozen in liquid nitrogen. Cells disruption was performed using a Mini Bead Beater (Biospec Products) at 3500 RPM for 20 seconds, in presence of glass beads (150–212 µm diameter) and 50 µl of TRI Reagent™ (Sigma Aldrich). Total RNA was then purified using the TRI Reagent™ (Sigma Aldrich), following the manufacturer's instruction, with minor modifications as follows: extracted RNA was washed twofold with 70% EtOH to reduce contamination from proteins and phenols. Total RNA concentration and purity were determined using a 100 UV–VIS spectrophotometer (Cary Series, Agilent

Technologies). cDNA was prepared from 1 µg of total RNA-template, previously treated with DNAse I kit (Sigma Aldrich). Retro-transcription was carried out using the Revert Aid Reverse Transcriptase cDNA kit (Thermo Fisher Scientific, Epson, UK), following the manufacturer's instructions. Quality of cDNA was routinely checked by standard PCR, before running real-time PCR.

RT-PCR and Real-Time PCR

cDNA was used as template for semi-quantitative RT-PCR, to measure the expression of the *ZEP* gene in both WT and ZEP over-expressor lines (Supplementary Figure S3). Primers used in RT-PCR are reported in the legend of Figure S3. *actin* was used as housekeeping gene.

Real-Time PCR was instead used to validate the robustness of the *ZEP* overexpression at the time of the biomass productivity measurements. Primers used were ATGGCGGAAGAAGATGTGCA and CCTTCAGCTCCTGGTCAAAG for actin and TCGTCGGCCTCATGATGACCA and GTTGGGTTGCAACTGTCGCTC for the *ZEP* gene. Real-time PCRs were performed with the SYBR green (5xHotFire Evagreen qPCR mix, Solis Biodyne, Tartu, Estonia) method in a CFX96 Touch Real-Time PCR Detection System (Bio-Rad Laboratories, Hercules, CA, USA). The cycling parameters were the following: 95 °C for 12 minutes, followed by 40 cycles at 95 °C for 15 seconds, annealing at 55° C for 20 seconds and extension at 72°C for 20 seconds. Results were analysed using the Pfaffl Method (5). Three biological replicates were always performed, and all reactions were carried out as technical triplicates.

Total proteins extraction

Cell pellets for total proteins extraction were collected via centrifugation from *Nannochloropsis* cultures in lab-scale photobioreactors (Supplementary Figure S6). 200 µl of Lysis D Matrix beads (MP Biomedicals) were added to the cell pellets, and samples were then flash-frozen, thawed, and treated with a bead beater using a MP FastPrep-24 5G, for 6.5 m/s for 60 seconds (MP Biomedicals). The freeze-thaw and bead beat cycle was repeated five times.

Afterwards, 120 µl of solubilization buffer (2% Lithium dodecyl sulphate, 30 mM Tris (pH 9), 30 mM Tris (pH 8), 60 mM DTT, 30% sucrose) were added to the disrupted cells, and the samples were incubated with shaking on a vortex for 30 min to solubilize. After solubilization, samples were centrifuged at 14,000 rpm for 5 minutes at RT, and the supernatant containing the total proteins extract was collected. Proteins were precipitated following the methanol-chloroform precipitation method, as previously described (6). Precipitated proteins pellets were submitted to the Vincent J. Coates Proteomics/Mass Spectrometry Laboratory at the University of California, Berkeley.

Mass Spectrometry and data analysis

Total protein extracts were analyzed on a ThermoFisher Orbitrap Fusion Lumos Tribid mass spectrometer equipped with an Easy nLC 1200 ultrahigh-pressure liquid chromatography system interfaced via a Nanospray Flex nanoelectrospray source. Samples were injected on a C18 reverse phase column (25 cm x 75 µm packed with ReprosilPur C18 AQ 1.9 µm particles). Peptides were separated by an organic gradient from 5 to 30% ACN in 0.02% heptafluorobutyric acid over 180 minutes, at a flow rate of 300 nl/min. Spectra were continuously acquired in a data-dependent manner throughout the gradient, collecting a full scan in the Orbitrap (at 120,000 resolution with an AGC target of 400,000 and a maximum injection time of 50 ms) followed by as many MS/MS scans as could be acquired on the most abundant ions in 3 s in the dual linear ion trap (rapid scan type with an intensity threshold of 5000, HCD collision energy of 32%, AGC target of 10,000, maximum injection time of 30 ms, and isolation width of 0.7 m/z). Singly and unassigned charge states were rejected. Dynamic exclusion was enabled with a repeat count of 2, an exclusion duration of 20 s, and an exclusion mass width of ±10 ppm.

Protein identification and label free quantitation were done with Integrated Proteomics Pipeline (IP2, Integrated Proteomics Applications, Inc. San Diego, CA) using ProLuCID/Sequest, DTASelect2 and Census (7–11). Tandem mass spectra were extracted into MS1 and MS2 files from raw files using RawExtractor (12). Data was searched against the PhycoCosm database (https://phycocosm.jgi.doe.gov/phycocosm/home) using the available genomic information for *Nannochloropsis gaditana*, supplemented with sequences of common contaminants and concatenated to a decoy database in which the sequence for each entry in the original database

was reversed (13). Search space included all fully tryptic peptide candidates with no missed cleavage restrictions. Carbamidomethylation (+57.02146) of cysteine was considered a static modification. We required one peptide per protein and both tryptic termini for each protein identification. The ProLuCID search results were assembled and filtered using the DTASelect program (9, 10) with a peptide false discovery rate (FDR) of 0.001 for single peptides and a peptide FDR of 0.005 for additional peptides for the same protein. The peak area corresponding to the log of the intensity for the signal of the ZEP protein (protein ID: 9828) was normalized to that measured for one internal standard, a core subunit of the 20S proteasome (protein ID: 1732), reported to be a stable eukaryotic cellular component under various conditions (14).

Design of the vector for the overexpression of genes of interest in Nannochloropsis

A modular vector to enable effective expression of genes of interest (GOI) in *Nannochloropsis* was developed, fusing a cassette conferring resistance to Zeocin (15), including the *Sh-ble* gene under the control of the endogenous constitutive UBIQUITIN promoter and the FCPA terminator from *P. tricornutum* (16), with a second cassette enabling the expression of specific GOIs. To achieve the desired vector modularity, all the regulatory elements controlling the expression cassette were surrounded by unique restriction sites, in order to facilitate the replacement of GOIs (Supplementary figure S13a). The endogenous LIPID DROPLET SURFACE PROTEIN promoter (*LDSP*, Gene ID: rna5756) was chosen as a strong regulatory element to drive the expression of the GOI, according to the expression of the *LDSP* gene that shows a four-fold higher value with respect to the endogenous constitutive UBIQUITIN promoter (17) (Supplementary figure S13b), together with the FCPA terminator from *P. tricornutum*. Although the functionality of the *LDSP* promoter to drive the expression of GOIs was already assessed in *Nannochloropsis oceanica* (18), its activity in *N. gaditana* has not been investigated yet. The region 5'-upstream of the start codon of the *LDSP* gene was chosen as the *LDSP* promoter and the region extending to the next upstream gene (Gene ID: rna5755) was cloned. When this sequence was used to drive the expression of the cassette conferring resistance to Zeocin, no colonies were obtained. Repeated rounds of transformation with progressively longer versions of the *LDSP* promoter extending towards the 3', up to include the first exon and intron of the *LDSP* gene, led to the identification of the sequence to get full functionality. PlantCARE (19) indeed predicted three TATA boxes in the final functional version of the promoter, belonging to the first intronic sequence, which might explain why the shorter versions of the promoter are not functional. The luciferase gene from *Renilla reniformis* and codon optimized for *Chlamydomonas reinhardtii* (20), *Crluc*, was used as a reporter gene to test the functionality of the expression cassette (Supplementary figure S13c). Zeo^R colonies were obtained and the presence of the *Crluc* gene integrated in the DNA was confirmed via colony PCR (Supplementary figure S13d). Luciferase activity was confirmed by monitoring the luminescence signal, validating the functionality of the expression cassette designed in this work in *Nannochloropsis* (Supplementary figure S13e).

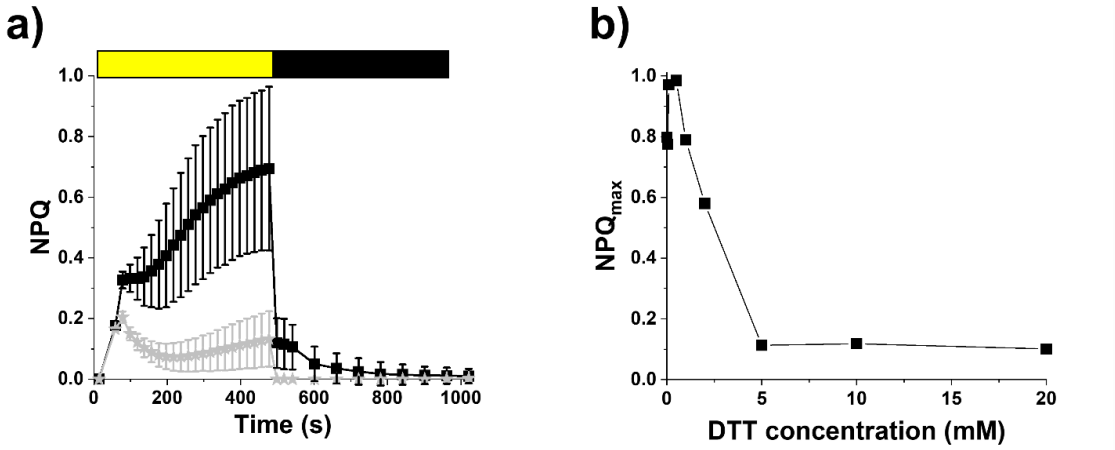

Fig. S1. Influence of zeaxanthin on NPQ activation in *Nannochloropsis*. a) NPQ induction analysis of *Nannochloropsis* cells grown at 100 µmol photons m^{-2} s^{-1}. Induction kinetics of untreated (black squares) and 20 mM DTT-treated (gray stars) samples are shown. The induction protocol consists of 8 min light at 800 µmol photons m^{-2} s^{-1} (yellow box) and 15 min of dark recovery (black box). Data are reported as average ± SD of 5 biological replicates. b) Titration of DTT impact on NPQ. NPQ is here expressed as maximal activity as a function of the concentration of DTT.

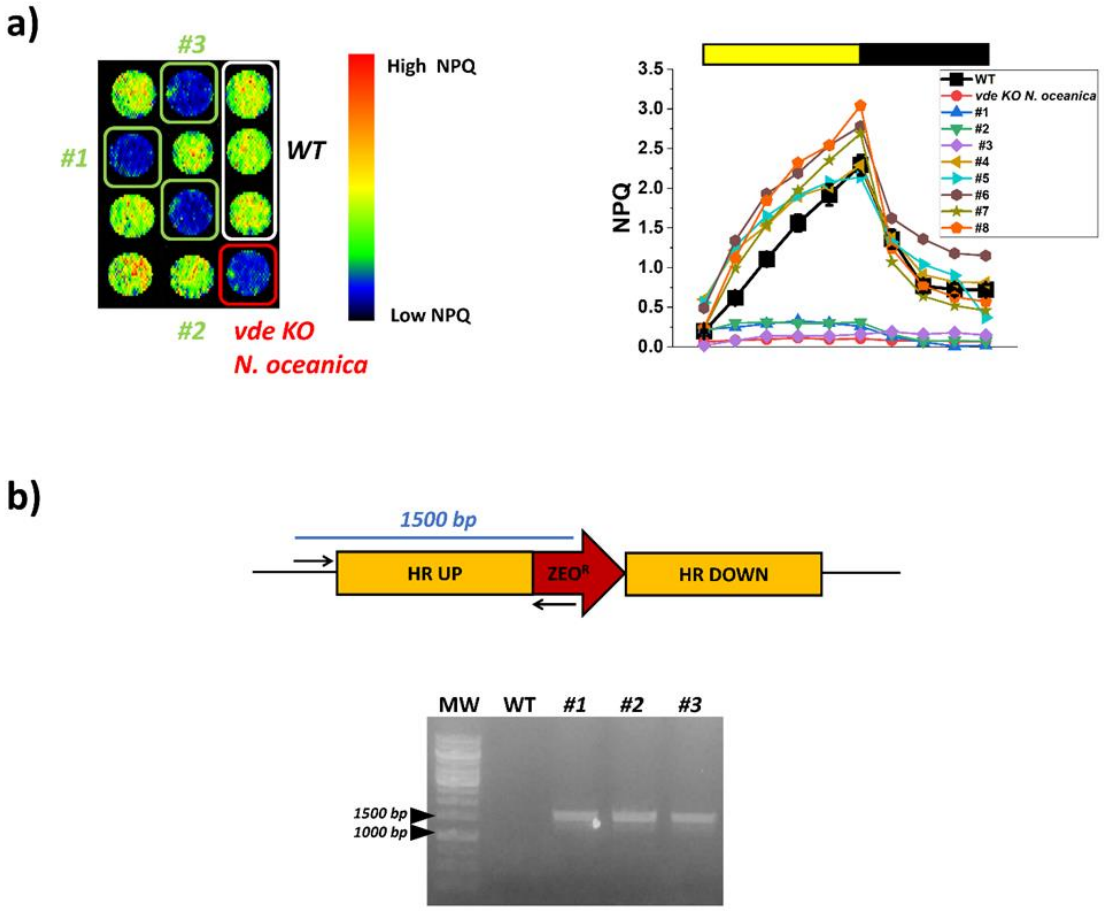

Fig. S2. Isolation of *vde KO* mutant in *Nannochloropsis gaditana*. VDE catalyses the conversion of violaxanthin to zeaxanthin, triggering the activation of Non-Photochemical Quenching (NPQ). a) KO mutants for the VDE protein (GENE ID: rna9604) show a defect in the NPQ response, as observed for the *vde KO* mutant of *N. oceanica*, used as control (21). On the left of panel a), a chlorophyll fluorescence image of an agar plate containing 12 spots corresponding to 8 mutant strains of *N. gaditana*, three copies of its parental strain (WT) and the *vde KO* mutant strain of *N. oceanica* is presented. *N. gaditana* strains #1, #2 and #3 show the photosynthetic phenotype of potential *vde KO* strains, as indicated by the lack of the NPQ response. Yellow and black boxes in the right panel a) indicate saturating light and dark exposure to investigate NPQ activation and relaxation kinetics, respectively.
b) *N. gaditana* strains #1, #2 and #3 resulted in genuine *vde KO* strains after validation of their genotype via colony PCR, by amplification of the left border of the integration locus. Primers For: CTGCTCCTCCCATTTCCCATG and Rev: GCATAATTAAAGCTATTCGGTCCAATTG used in the colony PCR of panel b anneal on the genomic sequence upstream of the 5'-homology region and on the zeocin resistance cassette, respectively. Amplification is expected only if the cassette is inserted in the expected genomic region. WT, wild-type.

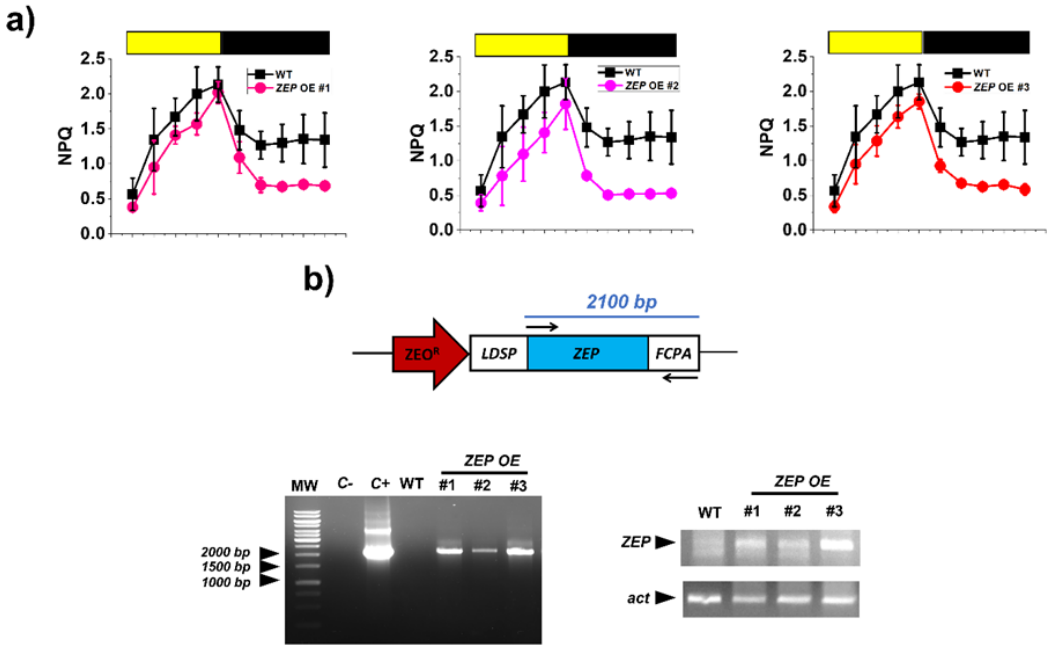

Fig. S3. Isolation of *ZEP OE* strain in *Nannochloropsis gaditana*. ZEP catalyses the conversion of zeaxanthin to violaxanthin, enabling the relaxation of Non-Photochemical Quenching (NPQ). A mutant strain overexpressing ZEP (*ZEP OE*) should show a faster relaxation of NPQ than the parental strain. a) NPQ kinetic of potential *ZEP OE* strains of *N. gaditana* during screening of a population of over-expressing strains, where a reduced NPQ activation and a faster relaxation is observed in mutants #1, #2 and #3 with respect to the parental strain. Yellow and black boxes indicate saturating light and dark exposure to investigate NPQ activation and relaxation kinetics, respectively. b) The genotype of the three strains was validated via colony PCR, by amplification of the portion of the cassette carrying the ZEP coding sequence together with the FCPA terminator. Primers For: ATGTTTTTCTTTTCTCAGACGT and Rev: TCAGTTGGGTTGCAACTGT used in the colony PCR. Strains #1, #2 and #3 resulted genuine *ZEP OE* strains of *N. gaditana* after validation of *ZEP* overexpression with respect to the parental strain via Reverse Transcriptase PCR (RT-PCR), by amplification of the *ZEP* coding sequence from the same amount of cDNA, as indicated by the similar amplification of the housekeeping gene for ACTIN (act). Strain #3 was chosen for most of the experiments of this work as it showed the greatest overexpression of the ZEP gene. Primers for ZEP amplification,
For: AGGTATGGTGCAACGTCTGG and Rev: CTGGCAGTACCACTTGTTCG
and primers for act amplification,
For: ATGGCGGAAGAAGATGTGCA and Rev: GTACAGGTCCTTGCGGATGT
used in the RT-PCR. WT, wild-type; C-, negative control using water as template; C+, positive control using the plasmid carrying the *ZEP* overexpression cassette.

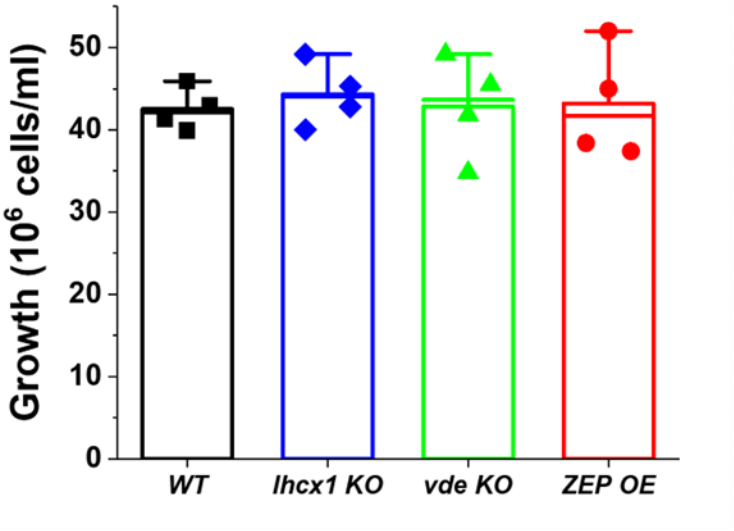

Fig. S4. Growth of the *N. gaditana* strains investigated in this work after 4 days in Erlenmeyer flasks. Strains were cultivated in F/2 at 100 µmol photons m^{-2} s^{-1}, supplemented with 10 mM $NaHCO_3$ to avoid carbon limitation, for 4 days, starting from a cell concentration of $5 \cdot 10^6$ cells/ml (see material and methods for details).

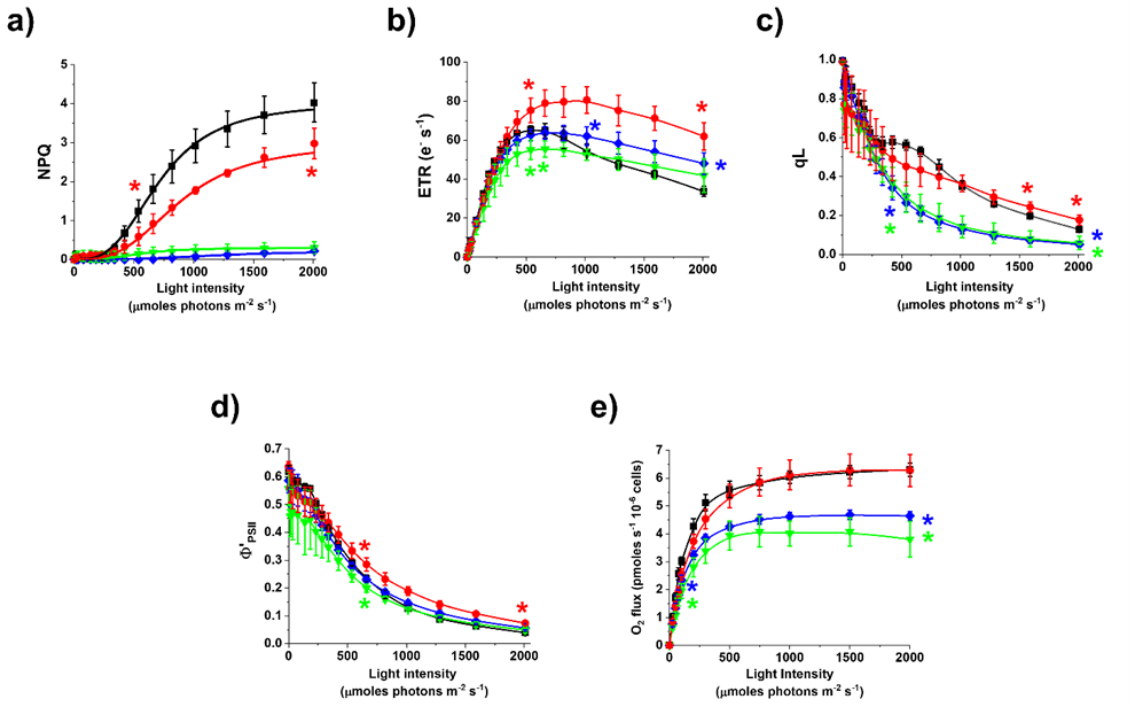

Fig. S5. Impact of the xanthophyll cycle on photosynthesis. The impact on photosynthetic functionality was assessed monitoring Chl fluorescence kinetics in vivo of liquid cultures cultivated in optimal light for 4 days (see materials and methods for details). a) NPQ activation, b) photosynthetic electron transport (ETR), c) photochemical capacity (qL), d) PSII quantum yield of illuminated cells (Φ' $_{PSII}$) and e) oxygen evolution at increasing irradiances. The same number of cells was used for the three measurements. WT *Nannochloropsis* strain, black squares; *lhcx1 KO*, blue diamonds; *vde KO*, green downward triangles; ZEP overexpressing strain, red circles. Data are expressed as average ± SD of four independent biological replicates. Asterisks indicate statistically significant differences between one single mutant (according to the color of the asterisk) and the parental strain, at a single time point (t-test, p-value<0.05). For each strain, all the data points between the two asterisks show statistically significant difference with respect to the WT.

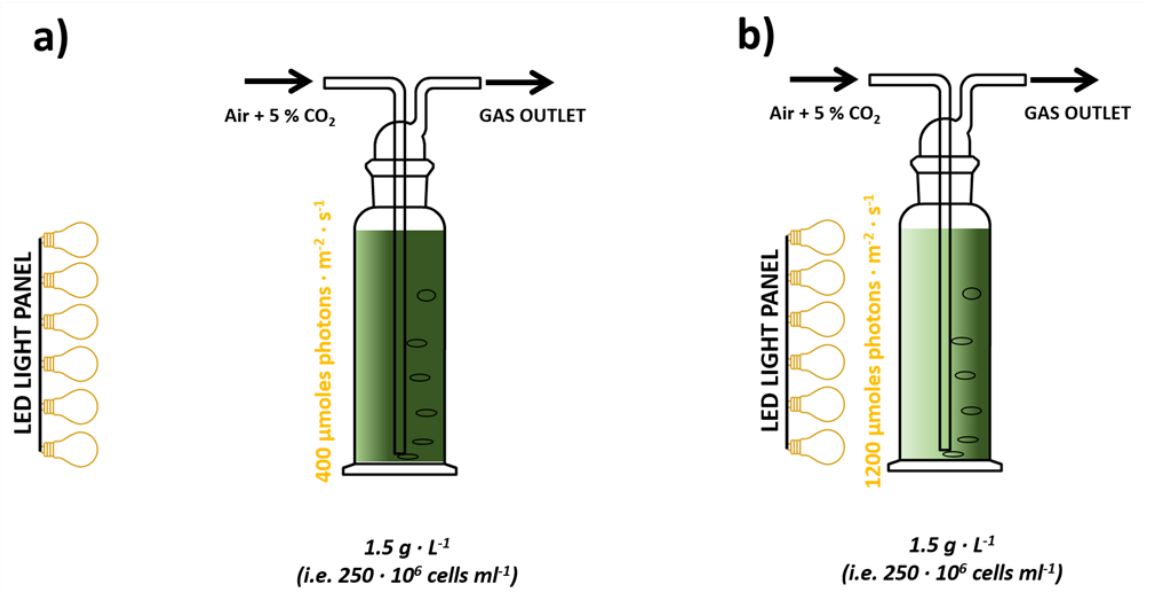

Fig. S6. Experimental set-up for semi-continuous cultures. *Nannochloropsis* cultivation was performed in Drechsel bottles starting from 1.5 g L^{-1} biomass concentration and cultures were diluted every other day to restore this value. Mixing and carbon source was provided through the insufflation of air enriched with 5% CO_2 (v/v), whilst light energy was provided with a LED panel from one side of the culture to get 400 and 1200 µmol photons m^{-2} s^{-1}, as indicated in a) and b), respectively.

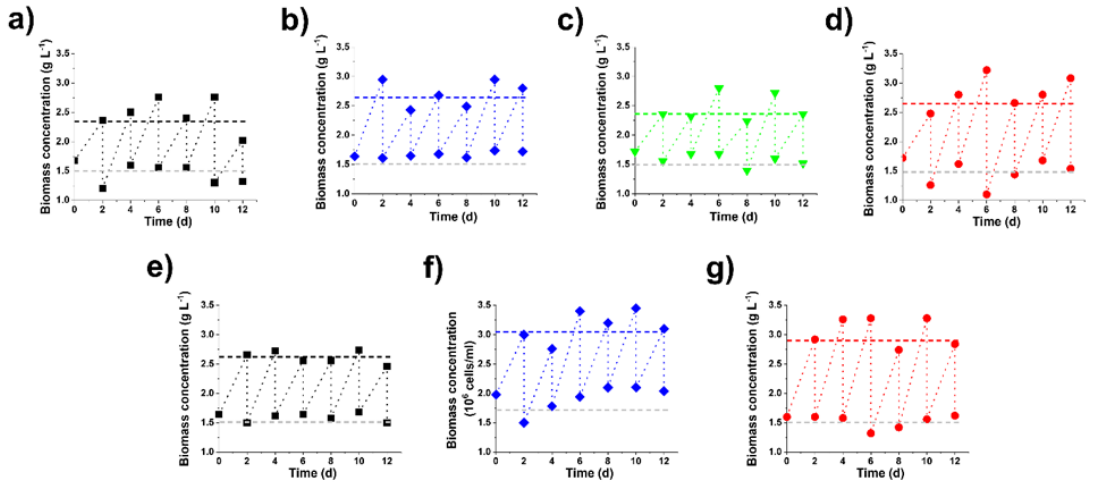

Fig. S7. *Nannochloropsis* semicontinuous cultures. Data were collected before and after dilution to restore the initial biomass concentration of 250 · 10^6 cells ml^{-1}, corresponding to 1.5 g L^{-1}, for *N. gaditana* WT (black squares, a and e), *lhcx1 KO* (blue diamonds, b and f), *vde KO* (green downward triangles, c) and ZEP over-expressor (red circles, d and g). Data at 400 and 1200 µmol photons m^{-2} s^{-1} are reported in a, b, c, d and e, f, g, respectively. Data for the *vde KO* at higher irradiance are not reported as the strain died in these conditions. All these panels show only a small timeframe of much longer sampling campaigns.

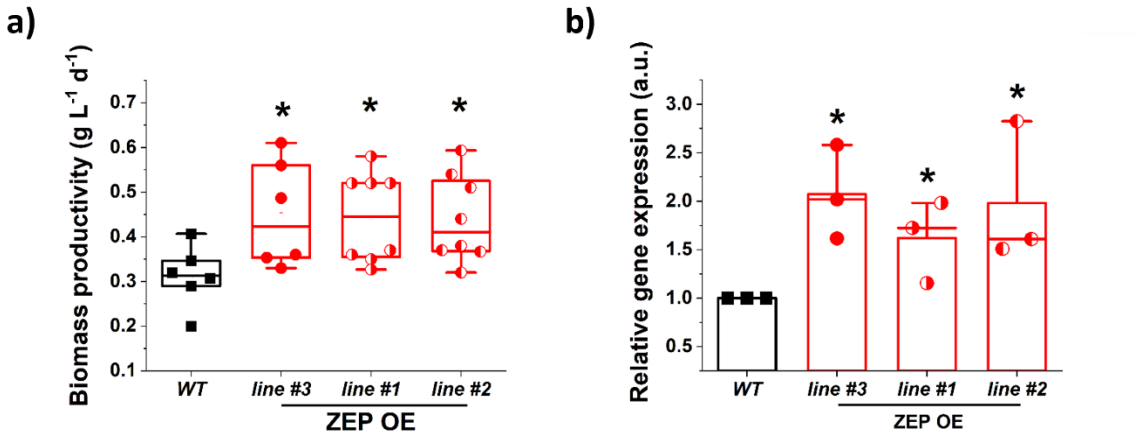

Fig S8. Biomass productivity and gene expression data. a) Biomass productivity of the other two ZEP overexpression lines isolated in this work (i.e. lines #1 and #2), compared to the WT and the ZEP over-expressor line presented in Figure 5 (i.e. line #3). Data indicates the average ± SD of at least six independent biological replicates.
b) Relative expression level of the *ZEP* gene, compared to the WT strain, at the time of the collection of the biomass productivity data, using the endogenous *ACT* gene coding for actin as reference. Please refer to the Supplementary Materials and Methods section for a detailed description of the protocol. Data indicates the average ± SD of three independent biological replicates. In both panels, asterisks indicate statistically significant differences between each ZEP over-expressor line and the WT. t-test, p-value < 0.05.

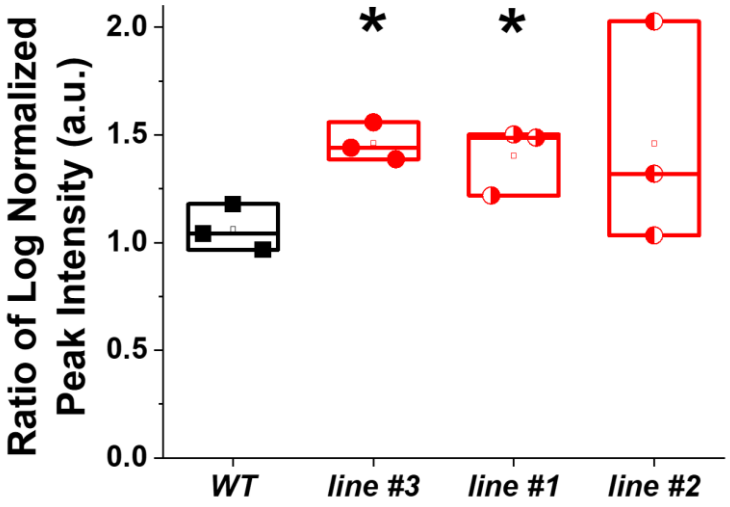

Fig. S9. Quantification of the ZEP protein in the three *Nannochloropsis* overexpressing lines with respect to the parental strain (WT) via Mass Spectrometry. Data indicates the average ± SD of three biological replicates collected during the experimental campaigns to assess biomass productivity in lab-scale photobioreactors. The log of the peak area corresponding to the intensity of the signal of the ZEP protein (Protein ID: 9828) was normalized to that measured for one internal standard (i.e. one of the core complex subunits of the 20S proteasome (14), protein ID: 1732, using PhycoCosm as reference, https://phycocosm.jgi.doe.gov/phycocosm/home), for each biological replicate. Asterisks indicate statistically significant differences between each ZEP over-expressor and the WT (t-test, p-value < 0.05). We acknowledge the Vincent J. Coates UCB Proteomics/Mass Spectrometry Laboratory (P/MSL) for support in running this analysis. Please refer to the supporting materials and methods section for details on proteins extraction and Mass Spec analysis.

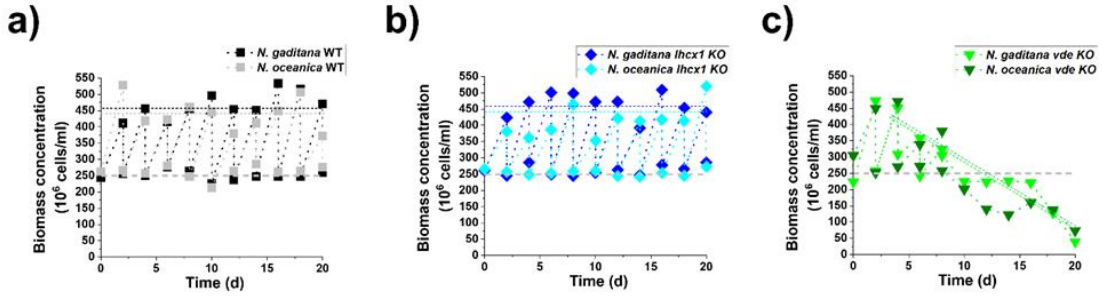

Fig. S10. Comparison between semi-continuous cultures of *N. gaditana* and *N. oceanica* strains. Data were collected before and after dilution to restore the initial biomass concentration of $250 \cdot 10^6$ cells ml^{-1}, corresponding to 1.5 g L^{-1} for the two parental strains (WT, a), *lhcx1 KO* (b) and *vde KO* strains (c). These data come from semi-continuous cultures at 1200 µmol photons m^{-2} s^{-1}. All these panels show only a small timeframe of much longer sampling campaigns.

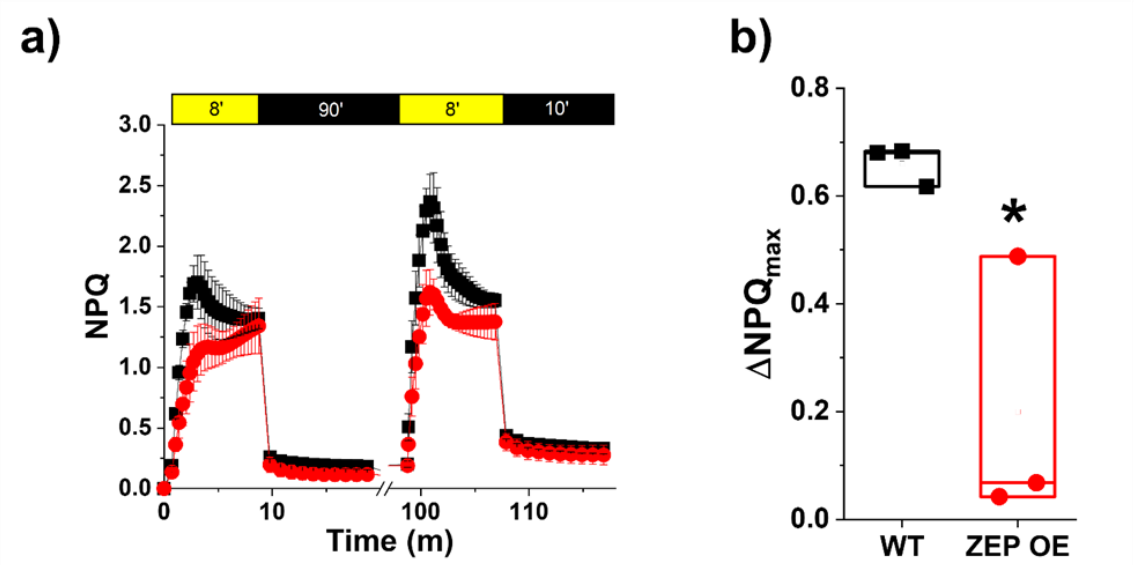

Fig. S11. Effect of ZEP over-expression on the contribution of zeaxanthin on NPQ. a) Chlorophyll fluorescence kinetics upon exposure of *Nannochloropsis gaditana* WT (black squares) and ZEP over-expressor (red circles) to two repetitions of 8 minutes light interspersed by 90 minutes dark. Yellow and black boxes indicate light and dark intervals, respectively. b) Difference in the maximum NPQ value between the second and first light treatment. Data are expressed as average ± SD of three independent biological replicates. Asterisk indicates statistically significant difference between ZEP over-expressor and parental strain (t-test, p-value<0.05).

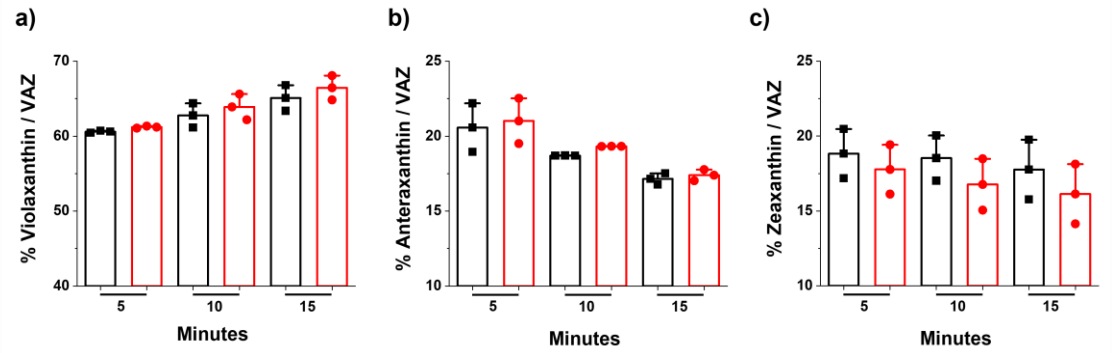

Fig. S12. Kinetics of conversion of zeaxanthin into violaxanthin. Data showing the content of the three xanthophylls in both WT and *ZEP OE* strains, after 5, 10 and 15 minutes of recovery in optimal light, after exposure to saturating light for 2 h. Data are expressed as average ± SD of three independent biological replicates.

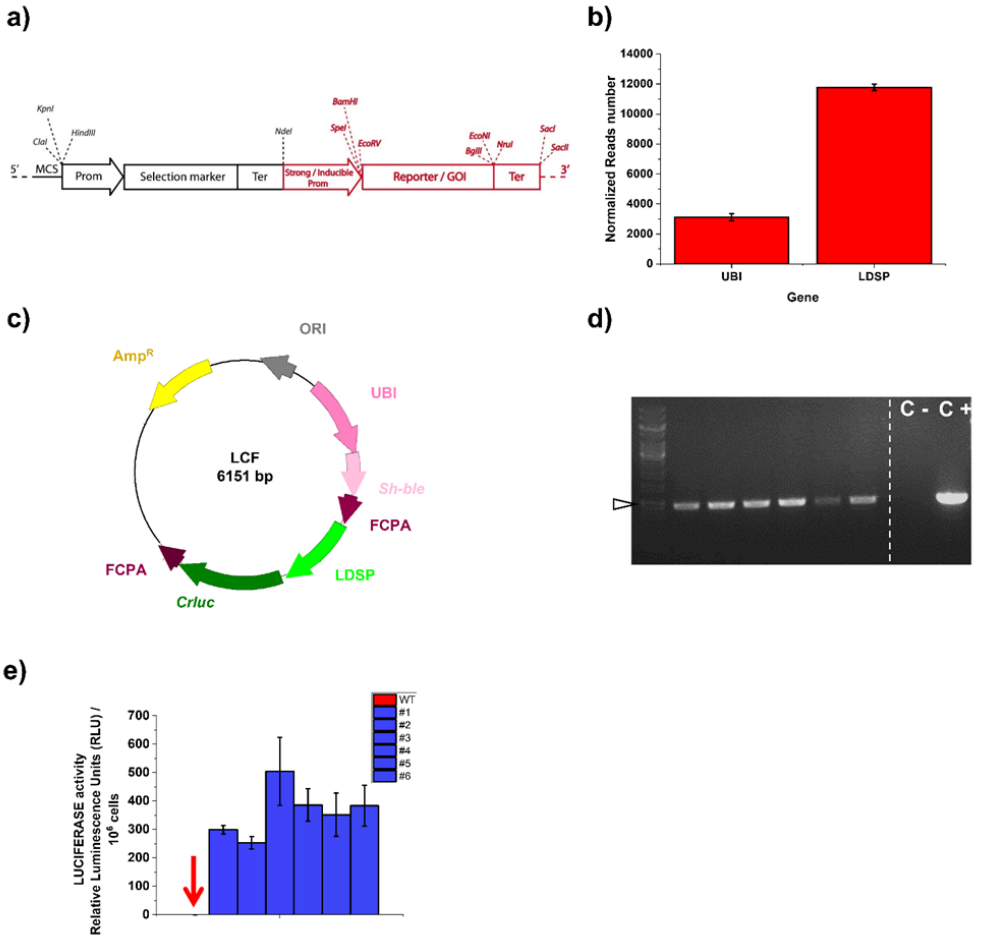

Fig. S13. Design of the construct for the overexpression of genes of interest in *Nannochloropsis*. a) Schematic overview of the construct, where the cassettes used for transformants selection (in black) and proteins over-expression (in red) are highlighted. Each element of the over-expression cassette was designed to be surrounded by unique restriction sites. This feature allows the simple opening of the vector for investigating molecular regulatory regions and for the replacement of the coding sequence of specific target proteins. Prom, Promoter; Ter, Terminator; GOI, Gene Of Interest. b) Normalized reads number for the UBIQUITIN (UBI) and LIPID DROPLET SURFACE PROTEIN (LDSP) genes from *N. gaditana* cells acclimated to 100 µmol photons m^{-2} s^{-1}. Data come from average ± SD of 3 biological replicates. c) Schematic overview of the vector (LCF) used to study the functionality of the LDSP promoter in *N. gaditana*. The backbone comes from the pBlueScript II SK (+) vector. The molecular components are depicted in different colors: yellow, Amp^R; grey, E. coli ORI; pink, endogenous UBIQUITIN promoter (UBI); light-pink, Sh-ble gene conferring resistance to Zeocin; violet, FCPA terminator; light-green, LDSP promoter; green, CrLUC gene. For ZEP overexpression, CrLUC was replaced with the endogenous ZEP coding sequence. d) *N. gaditana* transformants were tested via colony PCR, to validate the successful integration of the CrLUC gene (936 bp) in the genome. Six independent transformants (lanes 2 – 7) confirmed the presence of the CrLUC gene in their genome with respect to WT strains (C -). C -, WT *N. gaditana* strain; C +, plasmid DNA (LCF vector). The left and the right part of the picture come from different regions of the same agarose gel. The first lane indicates the molecular weight (MW) and the arrow indicates 1000 bp. e) LUCIFERASE activity of the six strains analysed in d). LUCIFERASE activity is expressed as Relative luminescence units (RLU) per million of cells. *N. gaditana* WT is indicated on the left of the series by a red arrow and measured values are negligible. Data are expressed as averages and SD of 3 biological replicates and indicate the functionality of the designed vector for effective protein overexpression in *N. gaditana*.

Table S1. Pigment content of *Nannochloropsis gaditana* after 2 h exposure to limiting (LL) and excess (EL) light conditions. Carotenoids are reported as mol/100 mol of Chl or, in the last three columns, normalized over the sum of the three xanthophylls violaxanthin (Vx), antheraxanthin (Ax) and zeaxanthin (Zx)(VAZ). Data are expressed as the average ± SD of 3 independent biological replicates. Asterisks indicate statistically significant differences between EL and LL conditions for each xanthophyll (t-test, p-value<0.05). Vaucheriax, Vaucheriaxanthin.

	VX	VAUCHERIAX	AX	ZX	B–CAR	% VX/VAZ	% AX/VAZ	% ZX/VAZ
LL	24.37 ± 2.41	4.88 ± 0.61	0.37 ± 0.53	0.99 ± 0.15	1.67 ± 2.37	93.84 ± 1.90	3.30 ± 0.33	3.96 ± 0.28
EL	18.12 ± 0.52*	5.09 ± 0.76	4.69 ± 1.37*	3.45 ± 0.83*	1.17 ± 1.66	70.32 ± 4.09*	17.72 ± 3.32*	13.29 ± 1.47*

346 **Table S2. Pigment content of *Nannochloropsis gaditana* strains investigated in this work.**
347 Data here reported come from cultures after 4 days of growth in optimal light (OL), 2 h treatment
348 with excess light (HL) and 1.5 h recovery in optimal light (ROL). Carotenoids are reported as
349 mol/100 mol of Chl. Data are expressed as the average ± SD of 4 independent biological replicates.
350 Vaucheriax, Vaucheriaxanthin.

351

	VAUCHERIAX			B–CAR		
	OL	**HL**	**ROL**	**OL**	**HL**	**ROL**
WT	21 ± 1.8	21 ± 1.85	21.5 ± 2.2	0.51 ± 0.37	0.48 ± 0.23	0.6 ± 0.7
lhcx1 KO	20 ± 2	20.4 ± 2.5	20.6 ± 3	0.75 ± 0.41	1.23 ± 0.76	1.2 ± 0.7
vde KO	21.2 ± 2.6	20.6 ± 1.8	24.5 ± 1.6	0.69 ± 0.5	0.58 ± 0.32	0.8 ± 0.6
ZEP OE	20 ± 1.5	19.5 ± 1.8	20 ± 2.8	0.8 ± 0.66	0.75 ± 0.35	1.26 ± 1

352
353

354 **Table S3. Pigment content of the strains investigated in this work cultivated in lab-scale**
355 **photobioreactors.** Chl concentration is expressed in picograms per cell (pg/cell). The sum of the
356 three xanthophylls, violaxanthin (V), antheraxanthin (A) and zeaxanthin (Z)(VAZ) is reported as
357 mol/100 mol of Chl. Low and High irradiance correspond to 400 and 1200 µmol photons m^{-2} s^{-1},
358 respectively. Data are expressed as the average ± SD, n > 10.
359

Species	Strain	Low Irradiance			High Irradiance		
		Chl (pg/cell)	Chl/Car	VAZ	Chl (pg/cell)	Chl/Car	VAZ
N. gaditana	**WT**	0.14 ± 0.01	2.73 ± 0.09	25.7 ± 1.15	0.07 ± 0.004	2.29 ± 0.16	23 ± 3.8
N. gaditana	***lhcx1 KO***	0.13 ± 0.02	3.12 ± 0.21	22.5 ± 2.22	0.05 ± 0.004	2.21 ± 0.03	22.2 ± 5.2
N. gaditana	***vde KO***	0.11 ± 0.01	2.9 ± 0.1	24.2 ± 1.08	/	/	/
N. gaditana	***ZEP OE***	0.16 ± 0.02	2.74 ± 0.04	23.5 ± 1.2	0.05 ± 0.004	2.17 ± 0.11	21.5 ± 4.3
N. oceanica	**WT**	0.13 ± 0.02	2.93 ± 0.24	24 ± 1.07	0.05 ± 0.008	2.05 ± 0.11	23.5 ± 5.4
N. oceanica	***lhcx1 KO***	0.1 ± 0.01	3.08 ± 0.22	22.2 ± 1.13	0.05 ± 0.003	2.2 ± 0.13	21.3 ± 5.7
N. oceanica	***vde KO***	0.13 ± 0.03	2.91 ± 0.08	23.4 ± 1.19	/	/	/

360

Table S4. Maximal photosynthetic efficiency (Φ_{PSII}) of the strains investigated in this work. Low and High irradiance correspond to 400 and 1200 µmol photons m^{-2} s^{-1}, respectively, n > 10.

Species	Strain	Low Irradiance	High Irradiance
N. gaditana	**WT**	0.63 ± 0.04	0.47 ± 0.04
N. gaditana	***lhcx1 KO***	0.64 ± 0.02	0.5 ± 0.02
N. gaditana	***vde KO***	0.6 ± 0.01	/
N. gaditana	***ZEP OE***	0.62 ± 0.01	0.4 ± 0.04
N. oceanica	**WT**	0.67 ± 0.04	0.48 ± 0.06
N. oceanica	***lhcx1 KO***	0.69 ± 0.03	0.46 ± 0.03
N. oceanica	***vde KO***	0.69 ± 0.02	/

Table S5. Photosynthetic activity expressed as oxygen evolution rate during the first fluctuation cycle of the protocol of figure 6a. The oxygen evolution rate is expressed as pmol O_2 s^{-1} 10^{-6} cells for all strains investigated in this work at 100, 300 and 15 µmol photons m^{-2} s^{-1}. Asterisks indicate statistically significant differences between each of the mutants and the parental strain at a specific light intensity (t-test, p-value<0.05).

Strain	**Irradiance**		
	100	**300**	**15**
WT	9.3 ± 1.4	12.45 ± 4.5	1.31 ± 0.17
lhcx1 KO	5.74 ± 1.63*	7.26 ± 2.7*	0.63 ± 0.19*
vde KO	12.7 ± 1.75	16.3 ± 7.45	1.35 ± 0.45
ZEP OE	9.5 ± 2.5	12.9 ± 5.3	1.19 ± 0.28

Table S6. Mathematical description of the oxygen evolution trends over the cycles of light fluctuation described in figure 6, for the *N. gaditana* strains investigated in this work. Trends observed in this experiment follow a linear function (y = b + ax) and the corresponding parameters for the different strains of this work are here reported. Data are expressed as the average ± SD of 4 independent biological replicates. Asterisks indicate when the slope of the linear function is statistically significant different from zero (t-test, p-value < 0.05).

	300				15			
	b	**a**	**Pearson's R**	**R-Square**	**b**	**a**	**Pearson's R**	**R-Square**
WT	15.07 ± 0.35	-0.59 ± 0.06*	-0.97	0.94	1.82 ± 0.04	-0.5 ± 0.01*	-0.99	0.99
Ihcx1 KO	7.8 ± 0.41	0.14 ± 0.08	0.56	0.32	0.85 ± 0.07	-0.11 ± 0.02*	-0.94	0.88
vde KO	16.25 ± 0.5	-0.03 ± 0.07	-0.18	0.03	2 ± 0.2	-0.48 ± 0.05*	-0.97	0.94
ZEP OE	14.8 ± 0.65	-0.3 ± 0.12	-0.7	0.48	1.83 ± 0.21	-0.35 ± 0.05*	-0.93	0.87

SI References

1. N. R. Baker, Chlorophyll fluorescence: a probe of photosynthesis in vivo. *Annu Rev Plant Biol* **59**, 89–113 (2008).

2. S. R. Starkenburg, *et al.*, A pangenomic analysis of the Nannochloropsis organellar genomes reveals novel genetic variations in key metabolic genes. *BMC Genomics* **15**, 1–21 (2014).

3. M. W. Fawley, I. Jameson, K. P. Fawley, The phylogeny of the genus Nannochloropsis (Monodopsidaceae, Eustigmatophyceae), with descriptions of N. australis sp. nov. and Microchloropsis gen. nov. *https://doi.org/10.2216/15-60.1* **54**, 545–552 (2019).

4. A. Bellan, “Genetic engineering approaches to increase microalgae light use efficiency.” (2018) (December 6, 2022).

5. M. W. Pfaffl, A new mathematical model for relative quantification in real-time RT–PCR. *Nucleic Acids Res* **29**, e45 (2001).

6. D. Wessel, U. I. Flügge, A method for the quantitative recovery of protein in dilute solution in the presence of detergents and lipids. *Anal Biochem* **138**, 141–143 (1984).

7. M. P. Washburn, D. Wolters, J. R. Yates III, Large-scale analysis of the yeast proteome by multidimensional protein identification technology. *Nat Biotechnol* **19**, 242–247 (2001).

8. T. Xu, *et al.*, ProLuCID: an improved SEQUEST-like algorithm with enhanced sensitivity and specificity. *J Proteomics* **129**, 16 (2015).

9. D. Cociorva, D. L. Tabb, J. R. Yates, Validation of Tandem Mass Spectrometry Database Search Results Using DTASelect. *Curr Protoc Bioinformatics* **16**, 13.4.1-13.4.14 (2006).

10. D. L. Tabb, W. Hayes McDonald, J. R. Yates III, DTASelect and Contrast: Tools for Assembling and Comparing Protein Identifications from Shotgun Proteomics. *J Proteome Res* **1**, 21–26 (2022).

11. S. Kyu Park, J. D. Venable, T. Xu, J. R. Yates III, A quantitative analysis software tool for mass spectrometry-based proteomics. *Nature methods* **5**, 319–322 (2008).

12. W. H. McDonald, *et al.*, MS1, MS2, and SQT—three unified, compact, and easily parsed file formats for the storage of shotgun proteomic spectra and identifications. *Rapid Communications in Mass Spectrometry* **18**, 2162–2168 (2004).

13. J. Peng, J. E. Elias, C. C. Thoreen, L. J. Licklider, S. P. Gygi, Evaluation of multidimensional chromatography coupled with tandem mass spectrometry (LC/LC-MS/MS) for large-scale protein analysis: The yeast proteome. *J Proteome Res* **2**, 43–50 (2003).

14. I. Sahu, *et al.*, The 20S as a stand-alone proteasome in cells can degrade the ubiquitin tag. *Nat Commun* **12**, 6173 (2021).

15. G. Perin, *et al.*, Generation of random mutants to improve light-use efficiency of Nannochloropsis gaditana cultures for biofuel production. *Biotechnol Biofuels* **8**, 161 (2015).

16. R. Radakovits, *et al.*, Draft genome sequence and genetic transformation of the oleaginous alga Nannochloropis gaditana. *Nat Commun* **3**, 686 (2012).

17. A. Alboresi, *et al.*, Light Remodels Lipid Biosynthesis in Nannochloropsis gaditana by Modulating Carbon Partitioning between Organelles. *Plant Physiol* **171**, 2468–82 (2016).

18. Y. Kaye, *et al.*, Metabolic engineering toward enhanced LC-PUFA biosynthesis in Nannochloropsis oceanica: Overexpression of endogenous Δ12 desaturase driven by stress-inducible promoter leads to enhanced deposition of polyunsaturated fatty acids in TAG. *Algal Res* **11**, 387–398 (2015).

19. S. Rombauts, P. Déhais, M. Van Montagu, P. Rouzé, PlantCARE, a plant cis-acting regulatory element database. *Nucleic Acids Res* **27**, 295–6 (1999).

20. M. Fuhrmann, *et al.*, Monitoring dynamic expression of nuclear genes in Chlamydomonas reinhardtii by using a synthetic luciferase reporter gene. *Plant Mol Biol* **55**, 869–81 (2004).

21. S. Park, *et al.*, Chlorophyll – carotenoid excitation energy transfer and charge transfer in Nannochloropsis oceanica for the regulation of photosynthesis. *Proc Natl Acad Sci U S A* **116**, 1–6 (2019).